Ideal unreactive metal/semiconductor interfaces: The case of Zn/ZnSe(001)

S. Rubini, E. Pelucchi, M. Lazzarino, D. Kumar,* and A. Franciosi†
Laboratorio Nazionale TASC-INFM, Area Science Park, Building MM, S.S. 14, Km. 163.5, I-34012 Trieste, Italy

C. Berthod,‡ N. Binggeli, and A. Baldereschi§
Institut de Physique Appliquée, Ecole Polytechnique Fédérale de Lausanne, CH-1015 Lausanne, Switzerland
(Received 21 December 2000; published 18 May 2001)

Zn/ZnSe(001) interfaces fabricated by metal deposition at room temperature onto ZnSe(001) $c(2\times2)$, 2×1, and 1×1 surfaces were studied by means of x-ray photoemission spectroscopy and current-voltage and capacitance-voltage measurements. All junctions exhibited an ideal unreactive behavior and an identical Schottky barrier height of 1.85 eV (for *p*-type conduction). *Ab initio* pseudopotential calculations for model interface configurations provide a microscopic explanation of the different behavior of Zn/ZnSe junctions as compared to Al/ZnSe and Au/ZnSe junctions.

DOI: 10.1103/PhysRevB.63.235307 PACS number(s): 73.40.Ns, 73.30.+y, 79.60.Jv, 81.15.Hi

I. INTRODUCTION

The physical mechanisms that control the band alignment at metal/semiconductor interfaces are still the subject of intense debate.[1–4] The recent application of state-of-the-art *ab initio* computational methods is producing stimulating results[5,6] for the few epitaxial metal/semiconductor contacts available.[7] Further important insight is being obtained by extending to metal/semiconductor interfaces linear-response-theory concepts used earlier in the study of heterojunction band offsets.[3,8] In particular, the relative importance of the chemical and structural properties of the two bulk materials comprising the junction and of interface-specific effects is finally being quantitatively assessed.

All such theoretical approaches, however, are hindered by the lack of experimental information on the local atomic configuration of the interface. Information is usually derived from the trends observed for simplified, model interface configurations. Common criticisms are that calculations for ideal, abrupt interfaces do not take into account atomic intermixing and defects, and also neglect the possible formation of interface reaction products. For example, in most B/AC interfaces involving a metal B overlayer and an AC compound semiconductor substrate, interface reactivity leads to a partial B-C exchange reaction in which the overlayer atoms react with the substrate anions (A), and the C cations displaced from the substrate are dissolved in the metal overlayer or segregated at the overlayer surface.[2] The interface heat of reaction calculated on the basis of the above phenomenology has been shown to correlate not only with the extent of atomic intermixing, but also in many cases with electronic properties as well.[2]

In view of the above complications, it is surprising that hardly any theoretical or experimental investigation has focused on metal/semiconductor interfaces where the semiconductor cation is also used to fabricate the metallic overlayer (C/AC). First, such common-cation metal/semiconductor junctions should minimize the interface heat of reaction, and may represent a class of ideal, unreactive interfaces. Therefore, they should be uniquely suited to experimental and theoretical studies of the influence of the interface configuration on the band alignment. Second, in common-cation junctions the nature of the metal overlayer unequivocally determines the chemical potential of the system, and this allows unambiguous theoretical determinations of the formation energies of the different interfacial configurations.

Along these lines, we present here comparative experimental and theoretical studies of Zn/ZnSe(001) interfaces. Junctions fabricated by molecular beam epitaxy (MBE) on different initial semiconductor surface reconstructions were investigated *in situ* by monochromatic x-ray photoemission spectroscopy using protocols especially suited to the study of common-cation interfaces. Selected junctions were also examined *ex situ* by current-voltage (I-V) and capacitance-voltage (C-V) measurements. Calculations of the electronic properties and formation enthalpies of the different interfacial configurations were performed using *ab initio* pseudopotential methods.

II. EXPERIMENTAL DETAILS

All junctions were fabricated in a MBE facility that includes twin solid-source growth chambers for III-V and II-VI semiconductors, a metallization chamber with effusion cells for metal deposition, and an analysis chamber with x-ray photoemission spectroscopy (XPS) capabilities, all interconnected via ultrahigh-vacuum transfer lines.

GaAs(001) 2×4 buffer layers 0.5 μm thick were initially grown at 600 °C on GaAs(001) wafers in the III-V MBE chamber after thermal removal of the native oxide. ZnSe epilayers 0.5 to 1 μm thick were subsequently deposited at 290 °C in the II-VI MBE chamber, with a typical growth rate of about 0.3 μm/h. ZnSe growth with a Zn/Se beam pressure[9] ratio of 0.4 or 1.0 was used to obtain Se-terminated 2×1 and Zn-stabilized $c(2\times2)$ surface reconstructions, respectively, as monitored by reflection high-energy electron diffraction (RHEED).[10,11] The two reconstructions are believed to correspond, respectively, to a fully dimerized monolayer of Se,[12] and to half a monolayer (ML) of Zn atoms on a complete ML of Se, i.e., to an ordered array of Zn vacancies within the outermost layer of Zn atoms.[13,14] The Se-rich 1×1 reconstruction, which involves submonolayer[15] or monolayer amounts[12,16] of excess Se on top of a fully Se-terminated (001) subsurface, was obtained here by depos-

iting Se onto ZnSe(001) 2×1 surfaces at room temperature for a few seconds, until the 2×1 reconstruction disappeared.

Samples fabricated for XPS studies included ZnSe epilayers doped with Cl from a $ZnCl_2$ source at variable levels in the $n=3\times10^{16}$ to $1\times10^{18}\,cm^{-3}$ range. Samples fabricated for *I-V* measurements included ZnSe epilayers with a graded doping profile, tailored in order to obtain a 300-nm-thick n^+ layer ($\sim4\times10^{18}\,cm^{-3}$) near the interface with the GaAs substrate and decrease the series resistance due to the ZnSe/GaAs heterojunction, while comparatively lower doping (3×10^{16} to $1\times10^{17}\,cm^{-3}$) was employed within a 500-nm-thick region at the interface with the metal.

After the ZnSe growth was completed, an elemental Zn flux (beam equivalent pressure 1.6×10^{-6} Torr) from an effusion cell was used to deposit elemental Zn on the desired substrate kept at room temperature. The RHEED pattern following Zn deposition indicated that the metal overlayer was polycrystalline.

Overlayers 0.3 to 5 nm thick were typically used for XPS studies of the interface chemistry and to determine the Schottky barrier height *in situ*. For this purpose the samples were transferred to the analysis chamber where a spectrometer employing a monochromatized Al K_α photon source (1486.6 eV) and a hemispherical analyzer were used to monitor the valence-band and core-level emission with an overall energy resolution of about 0.8 eV.

I-V and *C-V* measurements required *in situ* deposition of 100-nm-thick Zn overlayers onto the different ZnSe surfaces. A final Al layer was deposited *ex situ* to aid wire-bonding to the metal overlayer. Circular mesas with diameters in the 50–400 μm range were fabricated by standard photolithographic techniques to define the top contacts. Indium was used to fabricate the back contacts.

III. THEORETICAL METHODS

The *ab initio* calculations were performed within the local-density approximation (LDA) to density-functional theory (DFT), using the nonlocal pseudopotentials of Stumpf, Gonze, and Scheffler[17] and a plane-wave basis set. We used a 30 Ry kinetic-energy cutoff for the plane-wave expansion of the electronic orbitals, and the exchange-correlation potential was taken from the work of Ceperley and Alder.[18] A nonlinear core correction was used for Zn.[19]

Isolated Zn/ZnSe(001) interfaces were simulated using a slab geometry in supercells characterized by 17 semiconductor layers and 13 metal layers. We obtained epitaxial Zn/ZnSe(001) contacts by constraining the Zn atoms on fcc—as opposed to hcp—lattice sites. The Zn [001] axis was made parallel to the ZnSe [001] growth axis, and the Zn fcc lattice was rotated by 45° about the [001] axis relative to the cubic substrate in order to satisfy the epitaxial condition $a_\parallel = a_{ZnSe}/\sqrt{2}$, where $a_\parallel$ is the Zn in-plane lattice constant.

A similar epitaxial geometry was employed previously to simulate Al/GaAs(001) and Al/ZnSe(001) interfaces,[5,15,20,21] and is known to give rise to experimentally observed pseudomorphic structures, at least in the case of Al/GaAs(001).[22,23] In Al/GaAs and Al/ZnSe(100) junctions, the experimental lattice mismatch is about 1% ($\sqrt{2}a_{Al} > a_{GaAs} \approx a_{ZnSe}$), and produces a small elongation (2%) of the metallic overlayer in the [001] direction for pseudomorphic conditions. The atomic radius of Zn in a 12-fold coordinated metal structure ($r_{12}=1.39$ Å) is 3% smaller than that of Al ($r_{12}=1.43$ Å), and one therefore expects a contraction of the Zn overlayer along the [001] direction in pseudomorphic Zn/ZnSe(001) structures.

The macroscopic elastic deformation of the Zn(001) overlayer on the ZnSe(100) surface was determined by minimizing the total energy of a bulk Zn fcc metal with respect to the lattice parameter $a_\perp$ along the [001] growth direction, with the constraint $a_\parallel = a_{ZnSe}/\sqrt{2}$. We used the theoretical equilibrium lattice parameter $a_{ZnSe}=5.46$ Å (the experimental value is 5.65 Å). The calculations were performed in a four-atom tetragonal unit cell, using a (6,6,4) Monkhorst-Pack grid for the Brillouin zone integration.[24] The resulting lattice constant of the Zn overlayer along the growth direction was $a_\perp = 3.44$ Å. Our calculated equilibrium lattice constant for Zn is $a_{Zn}=3.67$ Å, which implies that the Zn overlayer contracts by 6% in our structures. This should be considered as an upper bound, as the polarization of the semicore Zn $3d$ electrons—not included in our computations—is expected to increase both the Zn and the ZnSe lattice constants, with a larger increase for Zn.

Along the lines of our previous study of the Al/ZnSe(001) system,[15] the interface atomic geometries were generated by selecting simple configurations that would give an ideal continuation of the semiconductor bulk, while taking into account the initial composition of the starting surface (see Sec. IV B). The structures that will be referred to as unrelaxed in the following include only the macroscopic elastic deformation of the Zn overlayer, with no local atomic relaxation at the interface. For these unrelaxed structures, we used as interplanar spacing across the metal-semiconductor interface the average of the interlayer spacings in the metal and in the semiconductor.

To evaluate the local atomic relaxation at the interface, we first considered metal/semiconductor structures with a thin Zn overlayer in contact with vacuum. The initial configurations prior to relaxation were generated by removing five atomic layers from the middle of the Zn slab in supercells containing the unrelaxed Zn/ZnSe structures. The atomic configurations were then fully relaxed, by incorporating the Hellmann-Feynman forces in a gradient procedure to minimize the total energy with respect to the ionic positions. Due to the presence of the vacuum, the metallic overlayer could freely relax along the growth direction, and release any residual stress in the junction. To examine the properties of the fully developed junctions, we then incorporated the resulting interplanar distances in a new supercell including a full Zn slab (13 layers of Zn). The interlayer spacings for the additional layers at the center of the Zn slab were set to the bulk value. We then let this structure relax again to allow for small readjustments in the metal. The supercell calculations for the metal/semiconductor structures were performed using a (6,6,2) Monkhorst-Pack grid for reciprocal-space integrations. A Gaussian broadening scheme with a full width at half maximum of 0.1 eV was used to take into account the partial filling of the bands.[25]

The *p*-type Schottky barrier height was written as[26]

$$\phi_p = \Delta E_p + \Delta V, \tag{1}$$

where ΔE_p is the difference between the Fermi level E_F of the metal and the valence-band maximum E_v of the semiconductor, each referenced to the average electrostatic potential of the corresponding crystal, and ΔV is the potential-energy lineup across the interface. The ΔE_p term was obtained from band-structure calculations for bulk, strained, fcc Zn and bulk ZnSe, using (16,16,16) and (8,8,8) Monkhorst-Pack grids to evaluate the charge density in the metal and in the semiconductor, respectively. The ΔV term was derived from the self-consistent supercell charge density via Poisson's equation, using planar and macroscopic averaging techniques.[3] ΔV is the only contribution to ϕ_p that is interface specific, and will depend, in general, on the atomic configuration established at the interface.

The values of ϕ_p calculated within the LDA framework were corrected to take into account many-body and relativistic effects. As discussed elsewhere,[3,15] ΔV should be accurately described by LDA-DFT, but ΔE_p may change substantially, mainly because of relativistic and self-energy corrections to the LDA band structure of ZnSe. Along the lines described in Ref. 15, we incorporated spin-orbit (-0.15 eV) and many-body ($+0.50$ eV) corrections to the position of E_v, resulting in an overall $+0.35$ eV increase in the *p*-type Schottky barrier ϕ_p relative to the LDA values. Because of the way the above correction was estimated,[15] it carries a substantial uncertainly, of the order of 0.2 eV. However, since it is a bulk-dependent correction, identical for the different interface configurations examined, it will not affect the *variations* in barrier height from one configuration to another. The estimated uncertainty for such variations is therefore of the order of our numerical accuracy, i.e., about 50 meV.

IV. RESULTS AND DISCUSSION

A. Experimental results

We monitored by XPS the emission from the Se $3d$, Se $3p$, and Zn $3d$ core levels, as well as the valence-band emission, from the different Zn/ZnSe(001) interfaces as a function of Zn coverage to rule out interdiffusion and gauge the Schottky barrier *in situ*. Relative to conventional metal/semiconductor photoemission studies, common-cation systems present some additional experimental challenges. In conventional photoemission studies the substrate cation core emission is most often used to gauge interdiffusion and determine the Schottky barrier height.[1,2] This is because its line shape and intensity are least affected by interface chemistry in the early stages of interface formation. In common-cation metal/semiconductor junctions, however, there is a partial superposition of substrate cation emission features and overlayer emission features, and the available XPS energy resolution is insufficient to separate the two core features with the necessary accuracy. Therefore, procedures based on the substrate anion core emission and the valence-band spectra have to be developed and tested.

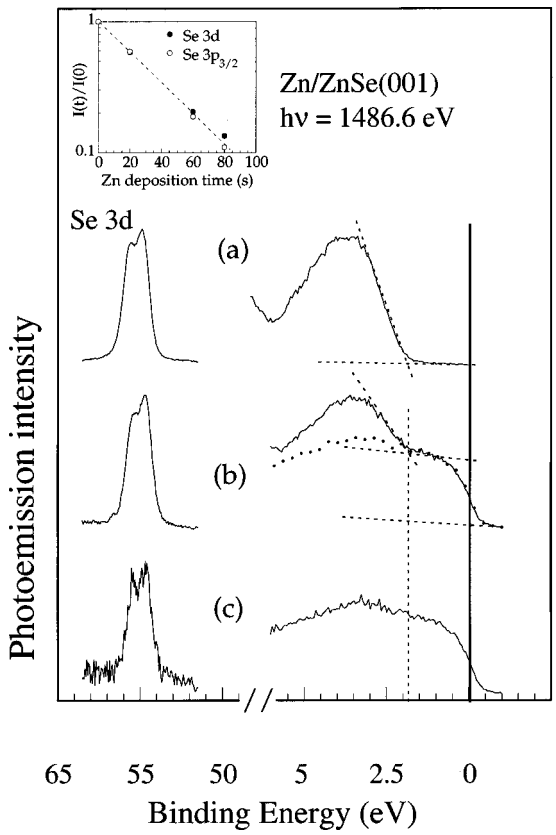

FIG. 1. Inset: Se $3d$ and Se $3p_{3/2}$ integrated photoemission intensity as a function of Zn deposition time during Zn deposition on ZnSe(001) 2×1 surfaces at room temperature. Se $3d$ (left) and valence-band photoemission (right) (a) from a ZnSe(001) 2×1 surface prior to Zn deposition; (b) following deposition of 2.4 nm of Zn; (c) following deposition of 4.0 nm of Zn. The zero of the energy scale corresponds to the Fermi level E_F of the spectrometer. At intermediate coverages the valence-band emission can be reproduced as a superposition of bulk like ZnSe (dashed line) and metallic Zn (solid circles) contributions.

As an example, we show in Figs. 1 and 2 selected results for Zn overlayers fabricated at 15 °C on the 2×1 surface reconstruction. In the inset of Fig. 1 we show in a semilogarithmic plot the integrated intensity of the Se $3d$ doublet (solid symbols) and Se $3p_{3/2}$ singlet (open symbols), normalized to the initial emission from the clean surface, as a function of Zn deposition time. Zn flux calibrations, and the observed exponential attenuation rate in Fig. 1, were consistent with layer-by-layer growth of the Zn overlayer at a rate of 0.04 nm/s, and unity sticking coefficient. The dashed line in the inset of Fig. 1 shows the expected ideal behavior for layer-by-layer growth in the absence of detectable interdiffusion.[27]

In the main body of Fig. 1 we show the Se $3d$ line shape (left) and the valence-band emission (right) from the ZnSe(001) 2×1 surface prior to metal deposition (a), and following deposition of 2.4 (b), and 4.0 nm (c) of Zn at 15 °C. The zero of the energy scale corresponds to the Fermi level of the spectrometer, E_F. The line shape of the Se $3d$ core levels remains unchanged with increasing Zn deposition, as expected in the absence of any relevant interface chemistry.

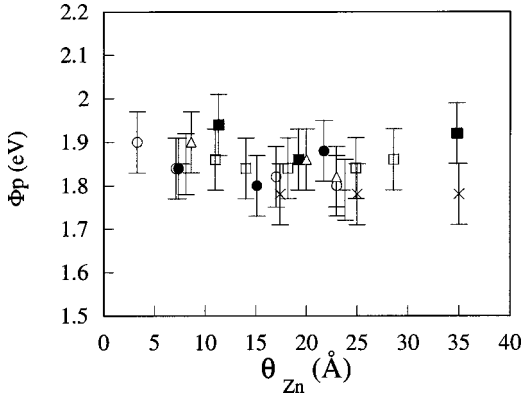

FIG. 2. XPS-determined values of the *p*-type Schottky barrier height ϕ_p as a function of Zn coverage θ for Zn/ZnSe junctions fabricated by Zn deposition on initial $c(2\times2)$ (crosses), 2×1 (open symbols), and 1×1 (solid symbols) ZnSe(001) surface reconstructions. Different symbol shapes correspond to different experimental runs.

From the ZnSe valence-band emission in Fig. 1(a) and a least-squares linear extrapolation of the leading edge (see dashed line), we determined the valence-band maximum E_v, and the position of the Se $3d$ centroid relative to E_v (53.24 ± 0.03 eV). The valence-band emission in Fig. 1(c) is indistinguishable from that of bulk Zn, with a well-defined Fermi-level cutoff with energy width consistent with the experimental resolution, as expected. At a coverage of 4.0 nm the Se $3d$ core intensity is reduced to less than 7% of the initial emission intensity, and the ZnSe valence-band emission, which scales accordingly, is effectively negligible in Fig. 1(c), so that the metallic Zn valence-band emission dominates.

At all intermediate coverages our results consistently showed that the valence-band emission can be reproduced by a superposition of a bulklike ZnSe emission and a bulk-Zn emission, shifted by a suitable energy relative to each other. This is exemplified in Fig. 1(b), where the dotted line shows the overlayer bulklike Zn emission, and the dashed line shows the leading valence-band edge of the substrate bulklike ZnSe emission. The resulting valence-band emission is consistent with the expected, ideal unreactive behavior of Zn/ZnSe(001) interfaces, and allowed us to read directly the energy separation between E_F and E_v in Fig. 1(b), i.e., the *p*-type Schottky barrier height $\phi_p=1.86\pm0.05$ eV.

The more conventional approach to Schottky barrier measurements monitors the position of substrate core levels unaffected by interface chemistry as a function of metal coverage to infer the position of the valence-band maximum E_v. Using for this purpose the measured Se $3d$ binding energy of 53.24 ± 0.03 eV relative to E_v, in Fig. 1(b) we would determine $\phi_p=1.82\pm0.07$ eV, consistent with the result of the previous determination.

The method of directly reading the band alignment from the superposition of bulklike substrate and overlayer valence-band emissions is suitable only for ideally unreactive interfaces, such as Zn/ZnSe(001), and at overlayer thicknesses comparable with the escape depth. Whenever it could be applied to the Zn/ZnSe(001) case, it confirmed the values obtained using the Se $3d$ core doublet. At relatively low and high Zn coverages as compared to the escape depth, only the latter method could be applied.

There is substantial evidence in the literature that the initial semiconductor surface reconstruction may influence the final value of the Schottky barrier height.[1,2] For ZnSe interfaces, in particular, Chen *et al.* have reported a 0.25 eV reduction in ϕ_p for Au/ZnSe(001) junctions fabricated on the 1×1 as opposed to the 2×1 surface reconstruction.[12] Lazzarino *et al.* recently found a 0.24 eV *p*-type barrier reduction when comparing Al/ZnSe(001) interfaces fabricated on ZnSe(001) 1×1 surfaces to those fabricated on $c(2\times2)$ and 2×1 surfaces.[15] This effect was associated with a local interface dipole created mainly by charge transfer from the first metal monolayer to the excess Se atoms at the interface, with a large relaxation in the Se-Se interatomic distances at the interface playing a major role in determining the value of the local dipole moment.[15]

We therefore repeated the type of studies summarized in Fig. 1 on interfaces fabricated through Zn deposition at room temperature on ZnSe(001) $c(2\times2)$ and ZnSe(001) 1×1 surfaces. Both types of interface showed an ideal unreactive behavior consistent with that exhibited by Zn/ZnSe(001)2×1 interfaces. For all three types of interface, XPS determinations of the *p*-type Schottky barrier height through the valence-band and core-level methods at different overlayer coverages are summarized in Fig. 2. Crosses, open symbols, and solid symbols denote results obtained following Zn deposition on ZnSe(001) $c(2\times2)$, 2×1, and 1×1 surfaces, respectively. Different symbol shapes correspond to different experimental runs, and the vertical error bars reflect the overall experimental uncertainty of ±0.07 eV. The resulting XPS-determined best values of the *p*-type Schottky barrier heights were $\phi_p=1.78\pm0.07$, 1.85 ± 0.07, and 1.86 ± 0.07 eV for the three types of interface. Such values are consistent with one another within the XPS experimental uncertainty.

To improve the accuracy in the determination of the barrier height and gauge the ideality of the corresponding junctions, we performed I-V and C-V measurements at 300 K on selected junctions. Typical I-V characteristics are shown in Fig. 3, where open circles, solid squares, and solid circles correspond to junctions fabricated through Zn deposition on ZnSe(001) $c(2\times2)$, 2×1, and 1×1 surfaces, respectively. The corresponding numerical values of the *n*-type Schottky barrier height ϕ_n and ideality factor n were $\phi_n=0.82\pm0.02$, 0.82 ± 0.02, and 0.83 ± 0.02 eV, and $n=1.07\pm0.01$, 1.07 ± 0.01, and 1.06 ± 0.01, respectively, for the three interfaces.[28] C-V measurements on the same samples (not shown) yielded only slightly higher values of the *n*-type barriers, i.e., $\phi_n=0.87\pm0.02$, 0.86 ± 0.02, and 0.89 ± 0.02 eV, respectively.

The transport results clearly rule out any Schottky barrier tunability. Taking $\phi_n\sim E_c-E_F\sim E_g-\phi_p$, where E_c is the conduction-band minimum in ZnSe, from the C-V transport values we would infer *p*-type barrier heights $\phi_p\sim1.83\pm0.02$, 1.84 ± 0.02, and 1.81 ± 0.02 eV, respectively, for interfaces fabricated on $c(2\times2)$, 2×1, and 1×1 surfaces. Within the combined transport and XPS experimental uncer-

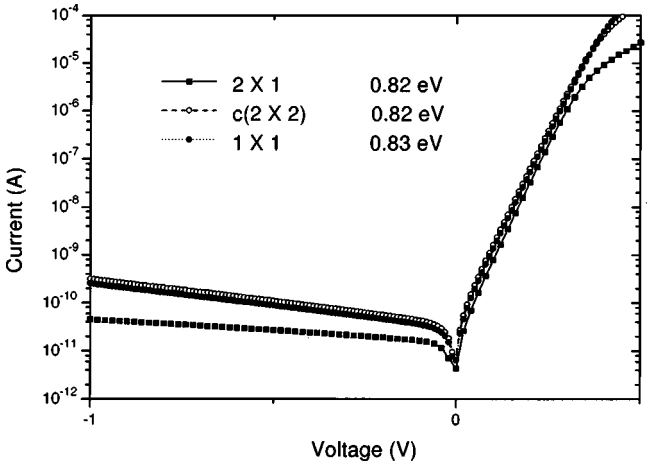

FIG. 3. Current-voltage characteristics for Zn/ZnSe junctions fabricated by Zn deposition on initial $c(2\times2)$ (open symbols), 2×1 (solid squares), and 1×1 (solid circles) ZnSe(001) surface reconstructions. The corresponding values of the *n*-type Schottky barrier height ϕ_n and ideality factor *n* are also shown.

tainties, such barrier heights are fully consistent with the results of the XPS studies in Fig. 2.

In summary, XPS and transport studies consistently show that the Schottky barrier height for ideal unreactive Zn/ZnSe(001) interfaces is independent of the initial reconstruction and composition of the ZnSe surface, in sharp contrast with the behavior exhibited by Au/ZnSe(001) and Al/ZnSe(001) junctions. A possible explanation is that the local interfacial configurations responsible for Schottky barrier tuning in Al/ZnSe(001) and Au/ZnSe(001) junctions correspond to more similar Schottky barrier heights in Zn/ZnSe(001). Alternatively, such configurations might simply not occur, i.e., might be unstable for Zn/ZnSe(001) junctions. Our calculations allowed us to discriminate between these two explanations.

B. Theoretical band alignment and interface formation energy

The simple unrelaxed atomic configurations selected for our calculations of the Zn/ZnSe(001) interface properties are illustrated in Fig. 4. For Zn overlayers fabricated on the $c(2\times2)$ surface we positioned the Zn atoms at the Zn vacancy sites of the outermost semiconductor layer. This results in a full layer of Zn atoms at the ideal zinc-blende position below the first fcc atomic layer of metallic Zn (see configuration *A* in Fig. 4). For Zn overlayers deposited on the 2×1 surface we terminated the semiconductor with a full layer of Se atoms at the ideal bulk zinc-blende positions and put the Zn atoms in the next layer on ideal fcc sites (configuration *B*). For Zn overlayers fabricated on the 1×1 surface, we used a virtual-crystal approach to terminate the semiconductor with a 50% Se–50% Zn atomic layer (see shaded symbols in Fig. 4) on top of the Se(001) subsurface layer (configuration *C*). The 50-50 composition was selected because the excess Se coverage of our 1×1 surfaces relative to the 2×1 surface was about 0.5 ML.[15]

The equilibrium interplanar spacings along the [001] growth direction, as obtained after full atomic relaxation, are

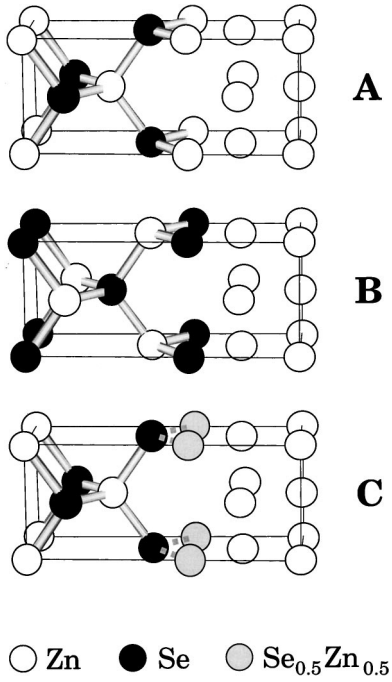

FIG. 4. Initial Zn/ZnSe(001) interfacial configurations employed in the supercell calculations, prior to atomic relaxation. Configuration *A* involves Zn atoms positioned at the Zn vacancy sites of the $c(2\times2)$ surface, below the Zn fcc lattice rotated 45° about the [001] axis relative to ZnSe to satisfy the epitaxial relation. Configuration *B* involves a ZnSe surface terminated by a full Se monolayer below the fcc metal. Configuration *C* involves a ZnSe surface terminated by a 50% Se–50% Zn atomic layer on top of a full Se monolayer.

illustrated in Fig. 5, for the three configurations examined. In the unrelaxed structures, each layer of Zn metal includes two inequivalent sublayers, with Zn atoms occupying either substitutional ($Zn^{(S)}$) or tetrahedral interstitial ($Zn^{(I)}$) sites in the continuation of the zinc-blende lattice. The relaxations of the $Zn^{(S)}$ and $Zn^{(I)}$ sublayers are different, and produce some buckling of the Zn(100) planes. The two sets of interplanar distances reported on the metal side of the junctions, in Fig. 5, correspond to the largest and smallest distances between relaxed Zn sublayers in adjacent planes.

The bulk interlayer spacings, denoted by solid horizontal lines in Fig. 5, are recovered only beyond the sixth (for configurations *A* and *B*) or the seventh (for configuration *C*) semiconductor layer and beyond the fourth (*C*) or fifth (*A* and *B*) metal layer from the junction. We note that convergence to the semiconductor bulk interlayer spacing is significantly slower here than in a system such as Al/GaAs(001), where the bulk value is already recovered beyond the second semiconductor plane.[29] Such a slow convergence is also observed in Al/ZnSe(001) junctions, and reflects the increased ionic character of ZnSe as compared to GaAs.

Except for the buckling in the metal, the largest changes in interlayer spacing as a result of relaxation concern the metal-semiconductor interlayer distance across the junction in configurations *A* and *B*, and the Se-$Zn_{0.5}Se_{0.5}$ interplanar separation in configuration *C*. The average separation between the last semiconductor layer and the first $Zn^{(S)}$ and

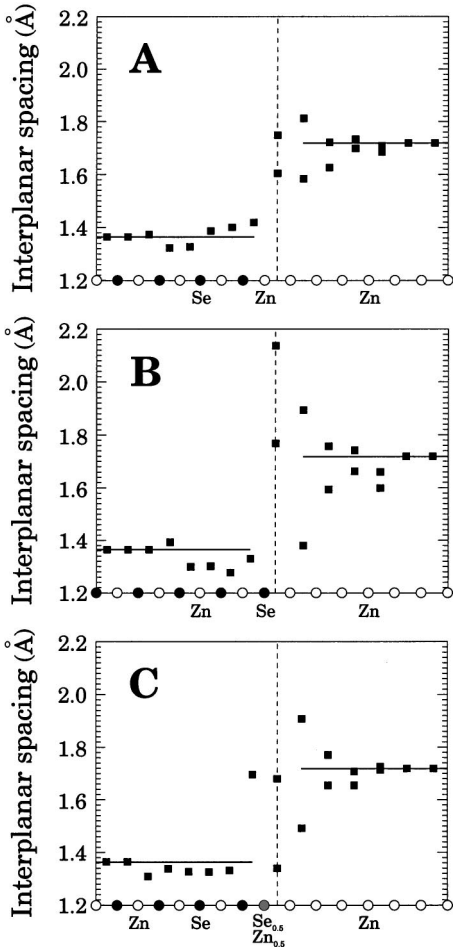

FIG. 5. Equilibrium interplanar spacings in Zn/ZnSe(001) junctions with interfacial configurations *A*, *B*, and *C*. The sequence of atomic planes prior to atomic relaxation is indicated at the bottom of each graph. Each Zn(001) plane in the unrelaxed structure includes two inequivalent sublayers; the two sets of interplanar distances reported in the plots, on the metal side of the junctions, correspond to the largest and smallest distances between relaxed sublayers in adjacent planes.

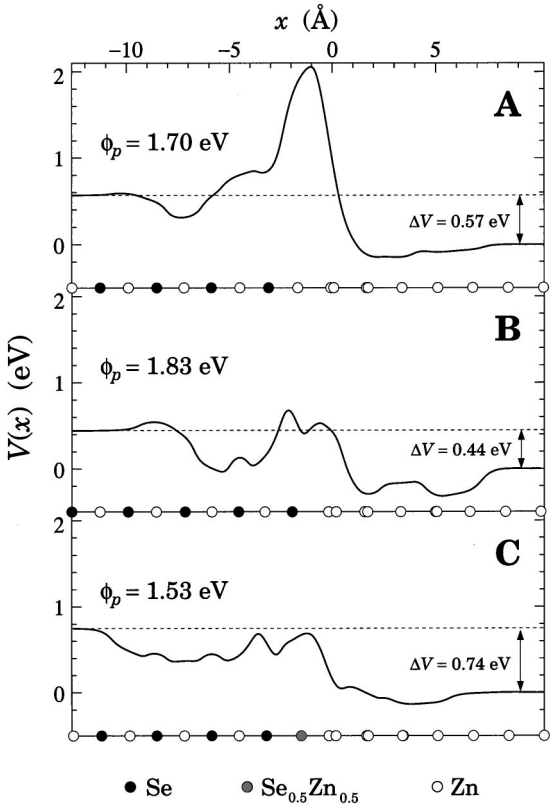

FIG. 6. Macroscopic average of the electrostatic potential energy V and potential energy lineup ΔV across the relaxed Zn/ZnSe(001) junctions. The negative sign has been omitted for clarity, and the calculated values are -0.57, -0.44, and -0.74 eV, respectively, for configurations *A*, *B*, and *C*. Relaxation is graphically illustrated at the bottom for each atomic plane. Double atomic symbols denote inequivalent relaxation at different sites. The calculated values of ϕ_p are also shown.

$Zn^{(I)}$ sublayers of the metal increases by 10% in configuration *A* and by 30% in configuration *B*, while the Se-$Zn_{0.5}Se_{0.5}$ interlayer distance increases by 25% in configuration *C*. Such changes relative to the unrelaxed geometries, which are quite substantial, are qualitatively similar to those observed in the Al/ZnSe(100) system, where relaxation yielded a 5% and a 20% increase in the average metal-semiconductor interplanar separation for configurations *A* and *B*, respectively, and a 40% increase in the Se-$Al_{0.5}Se_{0.5}$ interlayer distance for configuration *C*.[15]

In Fig. 6 we show the macroscopic average of the electrostatic potential V across the interface for the configurations *A*, *B*, and *C* examined after full atomic relaxation. The relaxed positions of the different (001) atomic planes are illustrated by the atomic symbols below each electrostatic potential profile. The horizontal dashed lines in Fig. 6 are used to illustrate the calculated electrostatic potential lineup ΔV across the three Zn/ZnSe(001) interfaces. We caution the reader that the negative sign has been omitted from ΔV in Fig. 6 for clarity, and that the calculated values are -0.57, -0.44, and -0.74 eV, respectively, for configurations *A*, *B*, and *C*.

The LDA values of the Schottky barrier height can be obtained from Eq. (1) using the above values of ΔV and the calculated LDA value of the band-structure term $\Delta E_p = 1.92$ eV. For configurations *A*, *B*, and *C* we obtained LDA *p*-type Schottky barrier heights of 1.35, 1.48, and 1.18 eV, respectively. Finally, by adding the combined relativistic and many-body correction of $+0.35$ eV, we estimated $\phi_p = 1.70$, 1.83, and 1.53 eV for the three configurations examined.

The predicted differences in barrier height are substantially larger than the experimental uncertainty in the determination of the barrier height. Therefore the three types of configurations that were used to explain the Schottky barrier tunability in Al/ZnSe(001) junctions,[15] if implemented in the case of Zn/ZnSe(001), should give rise to clearly detectable differences in the Schottky barrier height, in contrast with the experimental results in Figs. 2 and 3.

As to the absolute values of the calculated barrier heights, the large uncertainty carried by the many-body correction complicates comparison with experiment. Since the experi-

mentally observed *p*-type Schottky barrier value in Figs. 2 and 3 remains at about 1.85 eV irrespective of the initial reconstruction of the ZnSe(001) surface, predictions for both configurations *B* and *A* would be consistent with experiment. Finally, we note that the calculated trend in the barrier height with interface termination is different from that of the Al/ZnSe(100) system, where ϕ_p was found to decrease from 2.00 eV for configuration *A* (Se-$Zn_{0.5}Al_{0.5}$-Al interface) to 1.95 eV for configuration *B* (Zn-Se-Al interface), and to 1.39 eV for configuration *C* (Zn-$Se_{0.5}$-$Al_{0.5}$-Al interface).

The different trend is primarily the result of a large decrease in the calculated value of ϕ_p for configuration *A* in going from Al/ZnSe to Zn/ZnSe. A local interface dipole produced by the increased negative ionic surface charge of the Zn-terminated semiconductor surface in Zn/ZnSe relative to the $Zn_{0.5}Al_{0.5}$-terminated semiconductor surface in Al/ZnSe and the corresponding positive image charge in the metal cause the observed decrease.[30] Specifically, starting from Se-$Zn_{0.5}Al_{0.5}$-Al (configuration *A*) in Al/ZnSe(100), the local dipole generated by replacing the group-III Al atoms of the $Al_{0.5}$ sublayer at the interface with group-II Zn atoms decreases $\phi_p(A)$ by 0.6 eV. The subsequent replacement of the Al atoms in the metal overlayer with Zn atoms increases $\phi_p(A)$ by 0.07 eV, while atomic relaxation further increases $\phi_p(A)$ by 0.23 eV. The latter two contributions thus reduce only somewhat the effect of the local dipole, which is responsible for the change in the barrier trend.[31]

The formation energies E_f of the three Zn/ZnSe(001) interface configurations examined were calculated as

$$E_f = \frac{1}{2}\left(E_{\mathrm{tot}} - \sum_i n_i \mu_i \right), \tag{2}$$

where E_{tot} is the calculated total energy of the supercell, n_i and μ_i are the number of atoms and the chemical potential for each atomic species *i* in the supercell, and the $\frac{1}{2}$ factor takes into account that there are two equivalent interfaces within the supercell.

In a generic *B*/*AC* metal/semiconductor junction, there would be three atomic species and therefore three chemical potentials to contend with. The chemical potential μ_B and $\mu_{AC} = \mu_A + \mu_C$ can be obtained from the calculated total energy of the corresponding bulk materials, but this is not enough to specify all three of the *atomic* chemical potentials in Eq. (2). Because the supercell contains a different number of *A* and *C* atoms, the interface formation energy will depend linearly on the isolated *A* or *C* chemical potential. For a general *B*/*AC* interface, therefore, the relative stability of the different interfacial configurations depends on the isolated anion (or cation) chemical potentials, which, in turns, should be influenced by the experimental conditions. This very argument has been used recently to explain how the relative stability of As- and Ga-terminated Al/GaAs(001) and Al/Si/GaAs(001) interfaces could be determined by the growth conditions,[5,29] and to account for the wide experimental tunability of the corresponding Schottky barrier heights.[32–34]

In Zn/ZnSe(001), however, as for any other common-cation metal/semiconductor junction, the situation is intrinsically different. The chemical potentials μ_{Zn} and $\mu_{\mathrm{ZnSe}} = \mu_{\mathrm{Zn}} + \mu_{\mathrm{Se}}$ can be determined from the calculated total energies of bulk, strained fcc Zn and bulk ZnSe, respectively, and in thermodynamic equilibrium conditions they are sufficient to unequivocally define the interface formation energy in Eq. (2).

For the relaxed configurations *A* and *B* we obtained interface formation energies of 0.53 and 0.62 eV, respectively, per semiconductor interface atom. Although for the absolute values of our formation energies we estimated an uncertainty of 0.2 eV per semiconductor interface atom, *variations* in the formation energy between two configurations carry an uncertainty of only 0.01 eV per semiconductor interface atom. The implication is that configuration *A* is significantly more stable than configuration *B*.

Configuration *C* is of special interest, since for interfaces fabricated on the ZnSe(001) 1×1 surfaces charge transfer to the excess Se atoms at the interface has been associated with an important reduction of the *p*-type Schottky barrier height.[15] A reduction in ϕ_p is also observed in Fig. 6 when comparing the configuration *C* with configurations *A* and *B*. The corresponding calculated interface formation energy, however, is 1.90 eV per semiconductor interface atom. The more than threefold increase in interface formation energy relative to the other two interfaces makes it exceedingly unlikely that this interface would ever be encountered in practice.

We caution the reader that the above discussion is based solely on thermodynamic arguments, and neglects all possible kinetic effects associated with the growth of a Zn overlayer on ZnSe surfaces with different initial compositions. On the other hand, the calculated interface formation energies do capture the eminently reasonable trend that Se-rich semiconductor terminations are unlikely to remain stable under Zn deposition even at room temperature, and that the presence of a Zn flux during overlayer fabrication prevents the tunability of the interfacial configurations and of the Schottky barrier associated with the variable cation (or anion) chemical potential during interface fabrication.

V. CONCLUSIONS

Zn/ZnSe(001) metal/semiconductor junctions exhibit ideal unreactive properties, with layer-by-layer growth and no detectable atomic interdiffusion. Transport and photoemission measurements indicate a *p*-type Schottky barrier height of 1.85 eV, independent of the growth conditions and of the initial reconstruction and composition of the ZnSe(001) surface within experimental uncertainty. This is in contrast with the behavior of Au/ZnSe(001) and Al/ZnSe(001) contacts, which reportedly exhibit markedly lower *p*-type Schottky barrier heights for interfaces fabricated on the metastable Se-rich 1×1 surface.

The absence of any observable tunability of the Schottky barrier for Zn/ZnSe(001) is consistent with the calculated formation enthalpies of model interface configurations, which suggest that all Se-rich semiconductor terminations are unlikely to remain stable, and that the presence of a Zn

flux during overlayer fabrication prevents the tunability of the local atomic configurations associated with the variable cation (or anion) chemical potential.

ACKNOWLEDGMENTS

This work was supported in part by the National Science Foundation under Grant No. DMR-9819659, by the Commission of the European Communities under the ADDEV2000 Working Group program, and by the Swiss National Science Foundation under Grant No. 20-55811.98. D. K. acknowledges support by the International Center for Theoretical Physics in Trieste, Italy, under the TRIL program.

*Present address: Electronic Science Department, Kurukshetra University, 136119 India.

†Also with Dipartimento di Fisica, Università di Trieste, I-34127 Trieste, Italy.

‡Present address: DPMC, Université de Genève, 24 Quai Ernest-Ansermet, 1221 Genève 4, Switzerland.

§Also with Dipartimento di Fisica Teorica and INFM, Università di Trieste, I-34014 Trieste, Italy.

[1] *Electronic Structure of Metal-Semiconductor Contacts*, edited by W. Mönch (Kluwer, Dordrecht, 1990).

[2] L. J. Brillson, in *Handbook on Semiconductors*, Vol. 1, edited by P. T. Landsberg (North-Holland, Amsterdam, 1992), p. 281.

[3] M. Peressi, N. Binggeli, and A. Baldereschi, J. Phys. D **31**, 1273 (1998).

[4] G. Margaritondo, Rep. Prog. Phys. **62**, 765 (1999).

[5] J. Bardi, N. Binggeli, and A. Baldereschi, Phys. Rev. B **59**, 8054 (1999), and references therein.

[6] C. Berthod, N. Binggeli, and A. Baldereschi, J. Vac. Sci. Technol. B **18**, 2114 (2000), and references therein.

[7] C. J. Palmstrøm and T. D. Sands, in *Contacts to Semiconductors*, edited by L. J. Brillson (Noyes, Park Ridge, IL 1993), p. 67.

[8] See, for example, A. Franciosi and C. G. Van de Walle, Surf. Sci. Rep. **25**, 1 (1996).

[9] Beam equivalent pressures were monitored by an ion gauge located at the sample position.

[10] T. Yao and T. Takeda, Appl. Phys. Lett. **48**, 160 (1986).

[11] M. C. Tamargo, J. L. de Miguel, D. M. Hwang, and H. H. Farrel, J. Vac. Sci. Technol. B **6**, 784 (1988).

[12] W. Chen, A. Khan, P. Soukiassan, P. S. Mangat, J. Gaines, C. Ponzoni, and D. Olego, Phys. Rev. B **49**, 10 790 (1994).

[13] M. Vos, F. Xu, S. G. Anderson, J. H. Weaver, and H. Cheng, Phys. Rev. B **39**, 10 744 (1989).

[14] H. H. Farrell, M. C. Tamargo, and S. M. Shibly, J. Vac. Sci. Technol. B **8**, 884 (1990).

[15] M. Lazzarino, G. Scarel, S. Rubini, G. Bratina, L. Sorba, A. Franciosi, C. Berthod, N. Binggeli, and A. Baldereschi, Phys. Rev. B **57**, R9431 (1998).

[16] G. P. Lopinsky, J. R. Fox, J. S. Lannin, F. S. Flack, and N. Samarth, Surf. Sci. **355**, L355 (1996).

[17] R. Stumpf, X. Gonze, and M. Scheffler, Fritz-Haber-Institut Research Report No. 1, 1990 (unpublished).

[18] D. M. Ceperley and B. J. Alder, Phys. Rev. Lett. **45**, 566 (1980).

[19] S. G. Louie, S. Froyen, and M. L. Cohen, Phys. Rev. B **26**, 1738 (1982); in order to properly include the Zn nonlinear-core correction, the Zn pseudopotential was generated—with the parameters of Ref. 17—using the *same* atomic configuration $(s^{1.5},p^{0.25},d^{0.25})$ for each L component of the pseudopotential.

[20] R. G. Dandrea and C. B. Duke, J. Vac. Sci. Technol. B **11**, 1553 (1993).

[21] A. Ruini, R. Resta, and S. Baroni, Phys. Rev. B **56**, 14 921 (1997).

[22] A. Y. Cho and P. D. Dernier, J. Appl. Phys. **49**, 3328 (1978).

[23] G. A. Prinz, J. M. Ferrari, and M. Goldenberg, Appl. Phys. Lett. **40**, 155 (1982).

[24] H. J. Monkhorst and J. D. Pack, Phys. Rev. B **13**, 5188 (1976).

[25] C.-L. Fu and K.-M. Ho, Phys. Rev. B **28**, 5480 (1983).

[26] C. Berthod, N. Binggeli, and A. Baldereschi, Europhys. Lett. **36**, 67 (1996); C. Berthod, J. Bardi, N. Binggeli, and A. Baldereschi, J. Vac. Sci. Technol. B **14**, 3000 (1996).

[27] The expected functional form for the integrated intensity I of a substrate core level as a function of the overlayer thickness θ is $I(\theta)=I_0\exp(-\theta/\lambda)$, where I_0 is the initial intensity prior to metal deposition and λ is the effective escape depth of the photoelectrons. In the kinetic-energy range and experimental geometry of interest for the present study, the effective photoelectron escape depth was about 1.5 nm.

[28] See, for instance, D. K. Schroder, *Semiconductor Material and Device Characterization* (Wiley, New York, 1990), p. 130.

[29] C. Berthod, N. Binggeli, and A. Baldereschi, Phys. Rev. B **57**, 9757 (1998).

[30] The same microscopic mechanism also produces systematically larger ϕ_p values for anion-terminated than for cation-terminated semiconductor surfaces at abrupt polar metal/semiconductor junctions; C. Berthod, N. Binggeli, and A. Baldereschi (unpublished).

[31] We emphasize that atomic relaxation *per se* is not responsible for the change in the calculated barrier trend from the Al/ZnSe(100) to the Zn/ZnSe(100) system. Using for the Zn/ZnSe(100) system the same (relaxed) atomic geometries as for the Al/ZnSe system, we still find a lower *p*-type Schottky barrier height for the Zn/ZnSe A configuration than for the B configuration [$\phi_p(A)=1.47$ eV, $\phi_p(B)=1.82$ eV, and $\phi_p(C)=1.32$ eV].

[32] M. Cantile, L. Sorba, S. Yildirim, P. Faraci, G. Biasiol, A. Franciosi, T. J. Miller, and M. I. Nathan, Appl. Phys. Lett. **64**, 988 (1994); L. Sorba, S. Yildirim, M. Lazzarino, A. Franciosi, D. Chiola, and F. Beltram, *ibid.* **69**, 1927 (1996); G. Gigli, M. Lomascolo, M. De Vittorio, R. Cingolani, A. Cola, F. Quaranta, L. Sorba, B. H. Müller, and A. Franciosi, *ibid.* **73**, 259 (1998).

[33] S. De Franceschi, F. Beltram, C. Marinelli, L. Sorba, M. Lazzarino, B. Müller, and A. Franciosi, Appl. Phys. Lett. **72**, 1996 (1998); C. Marinelli, L. Sorba, B. H. Müller, D. Kumar, D. Orani, S. Rubini, A. Franciosi, S. De Franceschi, M. Lazzarino, and F. Beltram, J. Cryst. Growth **201/202**, 769 (1999).

[34] C. Marinelli, L. Sorba, M. Lazzarino, D. Kumar, E. Pelucchi, B. H. Müller, D. Orani, S. Rubini, A. Franciosi, S. De Franceschi, and F. Beltram, J. Vac. Sci. Technol. B **18**, 2119 (2000).